JOURNAL OF MECHANICAL ENGINEERING, SCIENCE, AND INNOVATION
ITATS
Research Article

Experimental Investigation of Heat Transfer in a Flat-Wall Impinging Diesel Spray Flame under Diesel-like Conditions

Journal of Mechanical Engineering, Science, and Innovation
e-ISNN: 2776-3536
2023, Vol. 3, No. 1
DOI: 10.31284/j.jmesi.2023.v3i1.4512
ejurnal.itats.ac.id/jmesi

Safiullah[1], Samir Chandra Ray[2], Iis Rohmawati[3], Rizal Mahmud[3]

[1]University of California, USA
[2]Bangabandhu Sheikh Mujibur Rahman Science & Technology University, Bangladesh
[3]Meiji University, Japan

Corresponding author:
Safiullah
University of California, USA
Email: safiull@uci.edu

Abstract

The heat loss through the walls of Internal Combustion Engines (ICEs) needs to be minimized and improved since it has a detrimental impact on the overall thermal efficiency of the engine. This study focuses on investigating heat transfer in a flat-wall impinging diesel spray flame, simulating diesel conditions, to optimize engine parameters. The effects of factors such as various injection pressures, nozzle hole diameters, impingement distances, and oxygen concentrations are analysed in combined and individually. Experimental techniques, such as high-speed imaging, heat flux sensors, and thermocouples, are used to visualize spray flame, measure heat flux profiles and temperature distributions, respectively. Preliminary results and their implications on heat transfer and heat loss are discussed. Regarding the parametric studies investigating the effect on wall heat loss under conditions similar to those of a small diesel engine, it was observed that the transferred heat on the wall was significant in certain conditions. These results emphasize the effectiveness of manipulating the injection rate profile as a viable step to suppress the heat transfer through the wall.

Keywords: *Heat transfer, diesel spray, injection pressure, nozzle hole diameter, impingement distance, oxygen concentration, similar injection rate*

Received: May 23, 2023; Received in revised: May 30, 2023; Accepted: May 31, 2023
Handling Editor: Ahmad Yusuf Ismail

INTRODUCTION

Road transportation has been a major contributor to CO_2 emissions [1], which presents a significant obstacle to achieving net-zero emissions and addressing climate

change. Despite the growing adoption of cleaner energy sources and electric vehicles, internal combustion engines (ICEs) remain widely sold, especially in 2030 [2]. Therefore, improving the thermal efficiency of ICEs is essential to reducing their environmental issue.

The heat loss reduction via the engine combustion chamber wall has garnered significant attention from researchers due to its potential as an effective method for improving thermal efficiency. Many attempts have been made to comprehensively understand heat transfer phenomena through an experimental measurement and simulations. Experimental studies have employed diagnostic techniques such as heat flux sensor measurements [3-6] and 2D visualization [7-8]. Furthermore, simulations have been utilized to model and analyze heat transfer processes, thereby enhancing our understanding of the phenomenon [9-11].

Recently, there has been a notable surge in research attention towards the installation of thermal barrier coatings (TBCs) in ICEs. This increased focus can be credited to advancements in coating technology and the utilization of advanced material properties. The findings of the study indicate that optimizing the thickness of TBCs is crucial, and thus, it has become a key parameter in their optimization [12]. A low-thermal-conductivity and low-thermal-capacity thermal insulation coating has been developed [13-15] to achieve a certain temperature swings. The utilization of TBCs materials that enable temperature swing holds great potential for enhancing the reciprocating ICEs performance without any negative impact on engine operation.

Furthermore, Uchida [16] conducted a review discussing the application of thermal barrier coatings as a means to enhance the thermal efficiency of internal combustion engines. The review also investigates the effects of TBCs on the performance and exhaust emissions of diesel, gasoline, and homogeneous charge compression ignition (HCCI) engines. Additionally, the article explores current advanced techniques and limitations regarding experimental and numerical analysis of the heat transfer mechanism, providing valuable insights into the future of TBC research.

On the other hand, parametric studies continue to play a pivotal role in examining the impact of various factors on thermal efficiency and heat loss. By systematically varying parameters such as injection pressure, nozzle design, fuel properties, and more, researchers are able to gain valuable insights into optimizing engine performance and minimizing heat loss [17-19]. These studies offer valuable information for enhancing thermal efficiency in a controlled and methodical manner.

Therefore, the aim of this research is to explore heat transfer in a flat-wall impinging diesel spray flame, simulating diesel conditions, across various parametric studies. Different injection pressures, nozzle hole diameters, impingement distances, and oxygen concentrations will all be investigated. Additionally, the potential combined effects of these parameters will be presented and discussed.

METHODS

Our earlier work [20-23] went into great depth regarding the experimental setup and settings. The experiment performed the use of a constant volume vessel (CVV), as illustrated in Figure 1. The vessel consists of four side windows as follows two for arranging an injector and an impinging wall opposite one another, and the other two for visualizing. The heater regulated the chamber temperature, and the chamber pressure was manually adjusted. The glass window and injector holder both have water-cooling tunnels built into them to keep them from overheating. Three K-type thermocouples were installed close to the wall, and one was placed between the nozzle tip and the wall. The heat flux measurement was conducted after a short delay following the hot gas feed to avoid turbulence in the CVV.

Table 1. Details of Experimental

	Non-Evaporation	Evaporation and Combustion
Ambient Gas Conditions		
Ambient gas	N_2	Evaporation: N_2 Combustion: Air (N_2:79%,O_2:21%) Air (N_2:84%,O_2:16%)
Pressure (MPa)	1.4	4.1
Temperature (K)	300	873
Gas density (kg/m^3)	16	←
Injection Conditions		
Injector type	Piezo actuator type	←
Number of nozzle holes	1	←
Injection quantity (mm^3)	5	←
Fuel	Diesel fuel	←
Nozzle holes diameter (mm)	0.133	0.101 0.122 0.133
Injection pressure (MPa)	120	58 68 80 120 171 180
Wall Conditions		
Wall material	Stainless steel	←
Impinging distance (mm)	40	30 40 50
Wall temperature (K)	300	460 ±10
Cooling method	-	Oil cooling

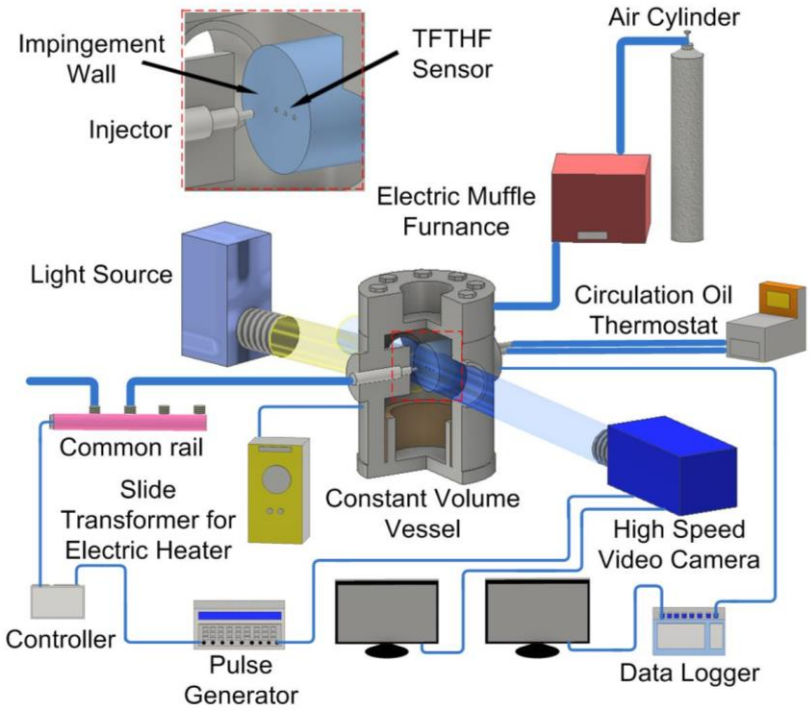

Figure 1. Experimental setup for high-speed imaging in constant volume vessel (CVV)

High-speed video camera (nac Image Technology Inc, HX-3) has been applied to capture the spray and flame behavior with an imaging speed of 20 kHz frames per second and a resolution of 320 x 448 pixels. The spray characteristics (non-evaporation and evaporation conditions) in the CVV had been illuminated by the Xenon lamp through a transparent quartz glass window on the side. To observe local temperature distribution, we employed a two-color technique [20].

Table 1 summarizes the experimental conditions. Diesel fuel was injected using a piezo actuator-type injector with a single-hole nozzle. The injection amount and timing

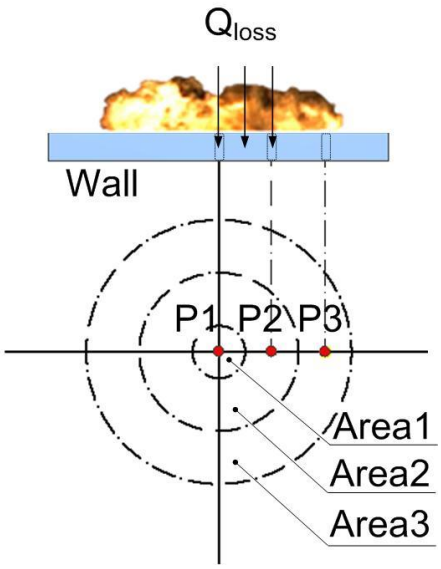

Figure 2. Areas and position of heat flux sensor

were controlled using a delay pulse generator. The injection was directed at an opposite direction to the impingement wall. The nozzle tip and the wall have been spaced by 30, 40, and 50 mm using spacers. Three thin film thermocouples heat flux (TFTHF) sensors are used to measure the instantaneous surface heat flux of the wall, similar to the previously calculated non-steady surface heat flux component [20]. The sensors were arranged radially, with a 10 mm space between them. The sensors' specified locations are Position 1, Position 2, and Position 3, which correspond to 0, 10, and 20 mm from the center of wall impingement, respectively. By integrating the heat flux over time and concentric regions, the overall heat transfer was estimated. As illustrated in Figure 2, the heat flux affecting certain areas was determined using concentric circles such as 0-5, 5-15, and 15-25 mm, which correspond to Area 1, Area 2, and Area 3, respectively.

RESULTS AND DISCUSSIONS

Heat Transfer Under Baseline Condition

In the following section, we will discuss high-speed video images of non-evaporation, evaporation, diesel flame soot luminosity, and flame temperature at a 40 mm wall impingement distance under baseline conditions. Additionally, we will present the local heat flux, heat transfer, and its ratio of heat loss to the total combustion heat. The injection pressure was set at 120 MPa, and the injection duration was 1.2 ms after the start of injection (ASOI). The oxygen concentration in the baseline condition was set at 21%.

A high-speed video camera's line-of-sight images are shown in Figure 3. Images of non-evaporating and evaporating wall impinging spray are shown in Figures 3(a) and (b), respectively. Each image shows the spray hitting the wall as it moves from top to bottom. Under the same ambient density (16 kg/m3), evaporating spray images as well as non-evaporating spray photographs were identified. In Figure 3(a), the non-evaporating spray was injected and impinged on the wall at 0.45 ms ASOI. The spray following impingement propagated radially to the circumferential wall region as the injection continued. When compared to before the spray impinged on the wall, mixture formation and air entrainment may be affected. The high ambient temperature, on the other hand, greatly reduced the liquid phase concentration in the evaporating spray in Figure 3(b), which encouraged spray atomization and the combination of air and fuel. The author has already addressed the additional discussion on mixture formation under non-evaporation and evaporation in a previous paper [27]. The amount of liquid spray is represented by the

white color's intensity. The liquid component of the spray did not reach the wall, as seen in the visual representation. This shows that a 40 mm impingement distance is enough to cause the liquid to turn into vapor before it reaches the wall. At 1.2 ms ASOI, the liquid phase almost completely evaporated, indicating the end of fuel injection.

The behaviors of impinging flame soot luminosity are depicted in Figure 3 (c). This figure illustrates the temporal evolution of impinging flame soot luminosity. In diesel engines, flame soot luminosity is primarily attributed to the thermal radiation emitted by soot particles within the flame, resulting in a broad emission spectrum. In the non-evaporating spray images showed in Figure 3 (a), soot luminosity were observed a few hundred microseconds after impinging spray on the wall, particularly at 0.9 ms ASOI. These flames subsequently vanished after 1.9 ms ASOI, as evidenced by the video images. The most intense luminosity was observed between 1.2-1.5 ms ASOI. Furthermore, upon visual examination of the non-evaporating spray photographs in Figure 3 (a), it becomes apparent that a luminous region existed within the vapor area as a result of combustion. This combustion occurred near the center of the wall impingement, where suitable equivalence ratios and temperatures facilitated ignition [28].

Figure 3 (d) shows the flame temperature distributions at an injection pressure of 120 MPa, obtained through two-color method analysis utilizing flame natural luminosity images. The temperature distribution trends closely mirror those of a flame since they are produced primarily from luminous regions and cannot be obtained from non-luminous parts. Temperature changes are represented by a color distributions scale ranging from dark to bright. The flame temperature distribution graphic depicts the highest flame temperature at 1.5 ms. During this timing, the maximum mean temperature is estimated to be approximately 2050 K.

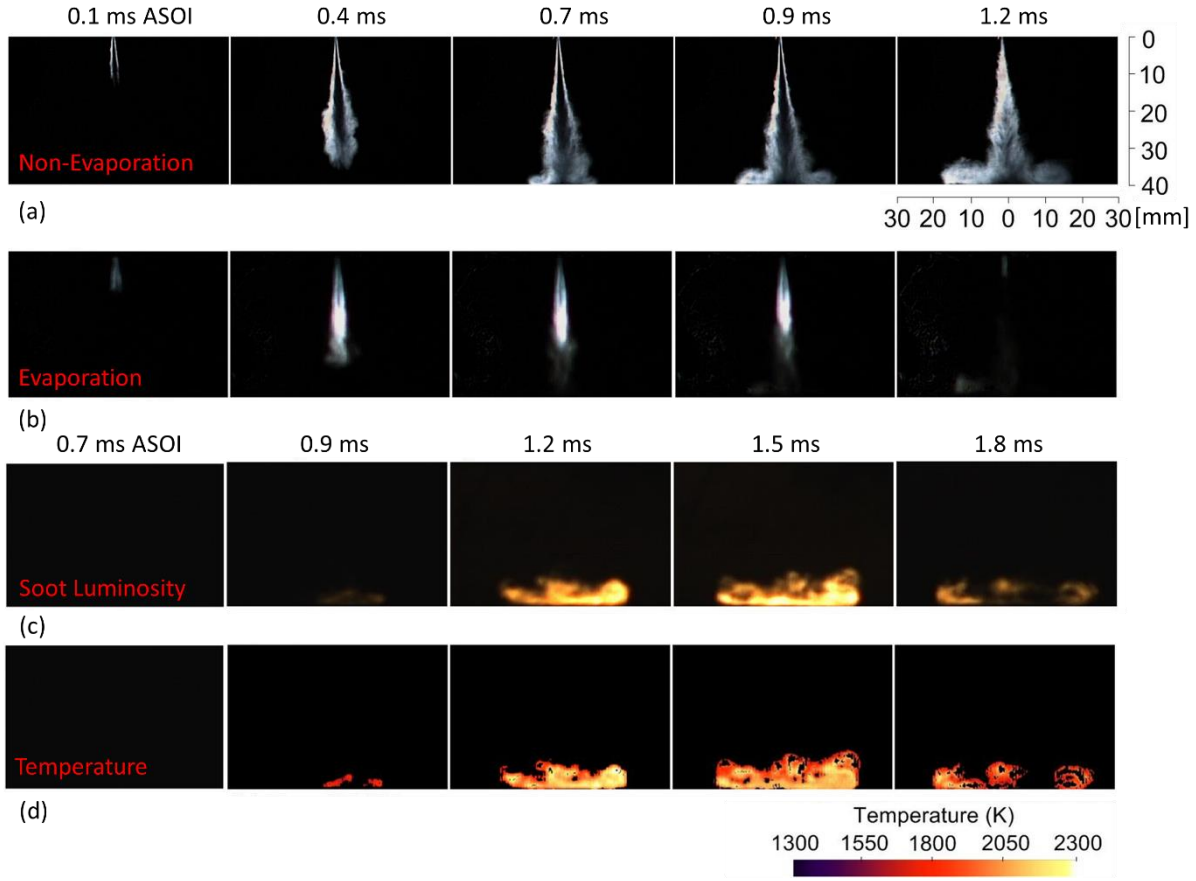

Figure 3. High speed video camera of non-evaporation (a), evaporation (b), flame soot luminosity (c), and flame temperature (d) at baseline condition

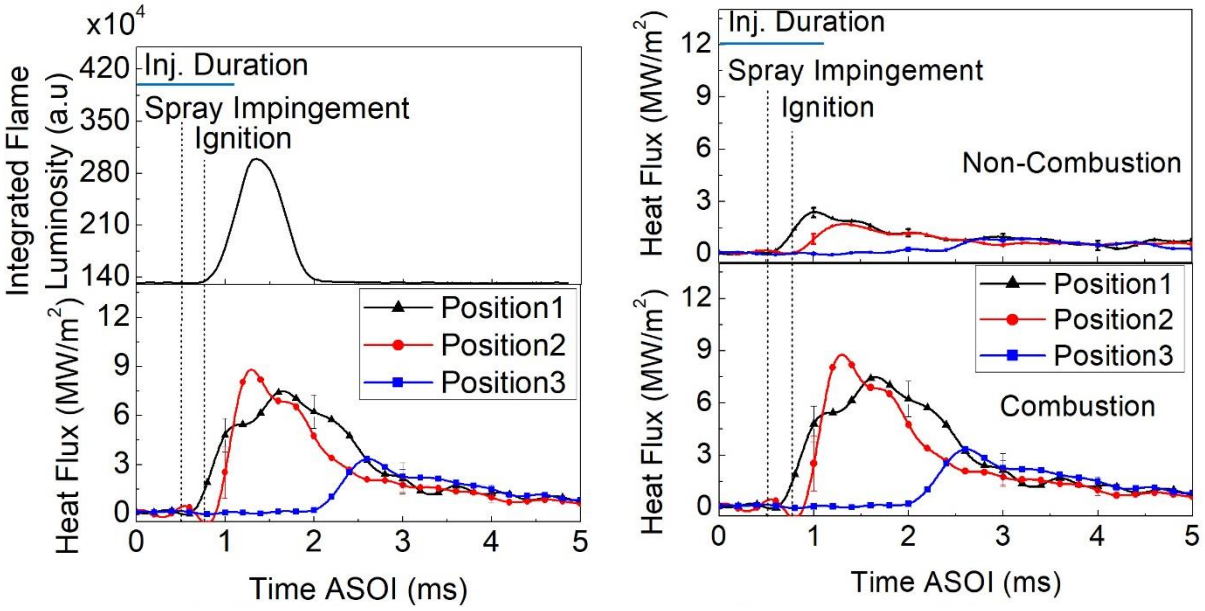

Figure 4. Local heat flux from TFTHF sensor and integrated soot luminosity (a) and local heat flux from TFTHF sensor under non-combustion and combustion conditions (b)

The heat transfer generated by the combustion flame to the impingement wall was investigated using an unsteady local heat flux and integrated flame luminosity. The integrated flame luminance was estimated by summing the red color values in natural flame color photographs, while temperature information from TFTHF sensors was used to determine the local heat flux. Figures 4 (a-b) show the results, with Figure 4 (a) showing the local heat flux (lower graph) and integrated flame soot luminosity (upper graph). Figure 4(b) also depicts the local heat flux under combustion (lower graph) and non-combustion (upper graph) circumstances. The spray impingement timings and ignition are also plotted on the graph. An increase in luminosity starts around the time of ignition.

The spatial temporal of local heat fluxes histories at the three measuring places (Positions 1, 2, and 3) could be seen in the local heat flux graph. These variations are caused by the non-uniformity of spray/flame motion in this region. Because the spray/flame travels radially after impingement, it arrives at all point at a various time, due to fluctuations in the heat flux. In all conditions, the local heat flux at Position 1 begins to increase first, followed by Positions 2 and 3. The convective effect when the turbulent component of the evaporating spray impinges on the wall might explain the early rise at Position1. The robust growth of the impinging flame from Position1 to Position2 can be attributed to the peak in local heat flux at Position2, as seen in Figure 3 (c-d). It is well understood that luminosity is strongly connected to soot volume fraction and temperature, with temperature having a substantial effect on heat transfer rate. Furthermore, due to wall friction and momentum loss induced by turbulent mixing, the local heat flow at Position3 is noticeably lower than at the other places. This local heat flux increases later than the other places because it takes time for the flame to reach Position3, which is positioned 20 mm from stagnation point of wall impingement.

As seen in Figure 4 (b), the waveform of the local heat flow changes substantially between combustion and non-combustion conditions. In the non-combustion (evaporate-

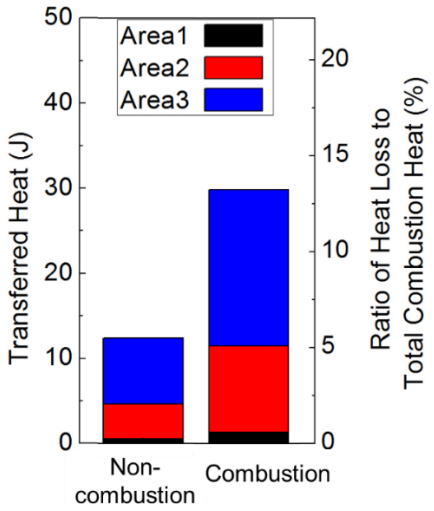

Figure 5. Heat transfer and heat loss ratio against the total combustion heat under non-combustion and combustion conditions

tion) case, the local heat flux has a simpler waveform than in the combustion case. This is a simple waveform because combustion does not occur in evaporation conditions. In this evaporation case, the local heat flux at Position1 decreases after the injection is completed.

Figure 5 compares transferred heat in different locations at injection pressures of 120 MPa for both non-combustion and combustion conditions. The left-side graph depicts the transferred heat on the vertical axis, while the opposite side of the graph depicts the heat loss to total combustion heat ratio. The fuel spray injection during the injection time caused convection, which was primarily responsible for the transferred heat value in the non-combustion condition of about 12 joules. The graph shows that the transferred heat increases as the area expands. This suggests that, despite the lower local heat flux value at Position3, a larger area in Area3 provides greater heat transfer to the wall, shown in Figure 4.

Regarding to combustion case, there is a substantial increase in the heat transferred because of the significant temperature difference between the flame gas and the wall. When comparing non-combustion and combustion conditions, convection of the non-combustion evaporating spray accounts for around 30-40% of the transfer of heat through the wall. Figure 5 depicts the ratio of total combustion heat loss to the wall, which accounts for approximately 13% of total combustion energy.

Heat Transfer Analysis at Various Injection Pressures, Nozzle Hole Diameters, Impingement Distances, and Oxygen Concentration Conditions

This section will discuss the correlation between injection pressure toward various parameters such as nozzle hole diameter, impingement total combustion, and oxygen concentrations for heat transfer analysis.

Figure 6 (a) exhibits the impingement distance/injection pressure combination and its relationship to total heat combustion. At different injection pressures (80, 120, and 180 MPa), three impingement distances (30, 40, and 50 mm) were used. The nozzle hole diameter was 0.133 mm. The following observations can be made regarding this combined impact as follows:

a) The heat transfer exhibited a significant increase, particularly at the highest injection pressure i.e. 180 MPa. This is seen as more evidence at a higher distance.

b) Apart from 180 MPa injection pressure, there are no significant heat transfer differences among the different impingement distances.
c) The heat loss ratio transferred to the wall is approximately 10-17% of total combustion energy.

The significant increase in transferred heat observed at the combination of a 50 mm impingement distance and 180 MPa injection pressure can be attributed to the longer impingement distance. This longer distance leads to an increase in the flame temperature at the time of impingement due to mixing, resulting in a substantial impact on both the local heat flux toward the total heat transferred. Previous studies conducted by [29-30] support this finding, showing an increase in the homogeneous flame temperature with an increase in impingement distance. Simultaneously, the higher injection pressure, which corresponds to a higher velocity, resulted in an increased flow velocity of the flame gas in the outer region. This higher velocity in the outer area contributed to the formation of a more pronounced waveform in the local heat flux and an overall increase in the total transferred heat.

On the contrary, a lower amount of heat was transferred when the impingement distance was 30 mm and the injection pressure was 80 MPa. This can be attributed to the significant impingement of liquid spray on the wall. Mahmud (5) stated that the liquid phase of the spray only reached to the wall at an impingement distance of 30 mm. In general, increasing injection pressure along with decreasing the presence of liquid phase on the wall [28]. The cooling effect caused by the liquid phase of fuel contributed to a slower rate of heat transfer, which was reasonable. It can be concluded that the existence of a liquid phase during impingement is effective to reduce the heat loss transferred to the wall.

Figure (6) described the various nozzle hole diameters of 0.122 and 0.133 mm with the injection pressures of 80, 120, and 180 MPa at a fixed impingement distance of 40 mm. As seen in Figure 6 (b), increasing of heat transfer is comparable with the injection pressure for both the nozzle hole diameters. The increase was gradual for the 0.122 mm diameter, while a significant increase in transferred heat was observed for the 0.133 mm diameter at higher injection pressures. As mentioned earlier, the increase in injection pressure contributes to higher flame velocities. The presence of high turbulent flow combustion, resulting from the combination of high injection pressure and larger heat transfer area, significantly influences the rate of transferred heat in the wall heat transfer under these conditions.

As shown in Figure (6), nozzle hole diameters of 0.133 mm and 0.122 mm were compared at injection pressure of 80 and 120 MPa. It can be seen that at 0.133 mm nozzle hole diameter has lower heat loss. Decreasing the dominant factor contributing to the heat loss at these injection pressures is the flame temperature which is inverse to the nozzle hole diameter [29]. However, at the highest injection pressure of 180 MPa, the 0.133 mm nozzle hole diameter resulted in higher heat loss compared to the 0.122 mm diameter. This is due to the high temperature of the end gases at the outer boundary of the flame during combustion. The temperature distribution was clearly observed to extend further along the wall, as evidenced by the data presented in Figure 7. The longer residence time of the flame in contact with the wall at the nozzle hole diameter of 0.133 mm and injection pressure of 180 MPa explains the further increase in transferred heat. However, in the case of a smaller nozzle hole diameter at 0.122 mm and higher injection pressure at 180 MPa, it led to increase in air entrainment and the fuel-air mixing will be accelerated then

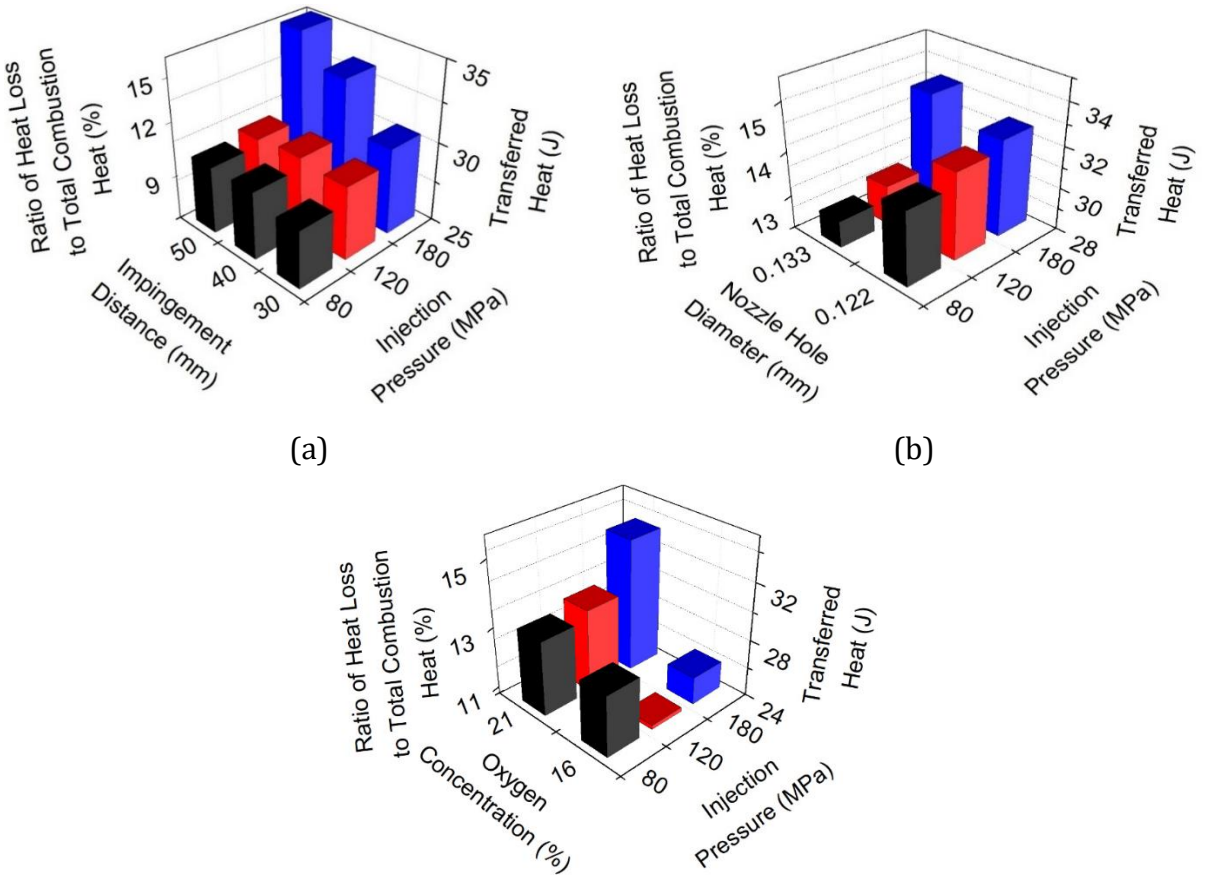

Figure 6. Heat transfer and heat loss ratio against the total combustion heat at various impingement distances (a), diameter nozzle holes (b), and oxygen concentrations (c) under injection pressure conditions

the rapid combustion occurs. Consequently, the residence time of the impinging flame along the wall decreased. According to Figure 6 (b), the heat loss ratio accounts for approximately 13-15% of the total combustion energy.

Figure 6 (c) illustrates the combinnation of oxygen concentration and injection pressure on the heat transfer and its ratio toward the total combustion heat. Different oxygen concentrations of 16 and 21% were investigated at three injection pressures (80, 120, and 180 MPa). The general effect could be described as follows: Firstly, at an oxygen concentration of 21%, increasing the heat transfer occurs at increasing injection pressure. However, this trend was not observed at an oxygen concentration of 16%, as the transferred heat did not increase proportionally despite higher injection pressures. This suggests that the dominant factor influencing transferred heat is not solely the high velocity resulting from increased injection pressure when the oxygen concentration is below 21%. Secondly, reducing the heat transfer to the wall generated consistently lower oxygen concentrations across all cases. This decrease can be attributed to the lower flame temperature associated with lower oxygen concentrations. Contrarily, stable combustion occurs at the higher oxygen concentration of 21%, resulting in a higher flame temperature and subsequently a greater heat transfer rate [30]. Thirdly, the ratio of heat loss to the wall is approximated 10-15% of the total combustion energy.

In terms of the combined effect, reducing the heat transfer to the wall generated consistently lower oxygen concentrations across all cases due to the lower flame tempera-

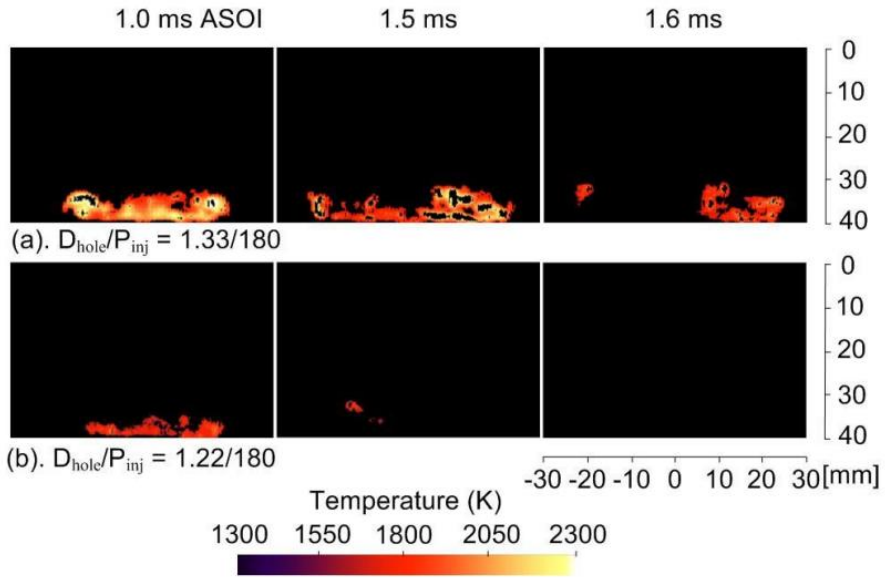

Figure 7. Comparison of temperature distribution at 0.122 and 0.133 mm nozzle hole diameter under an injection pressure of 180 MPa.

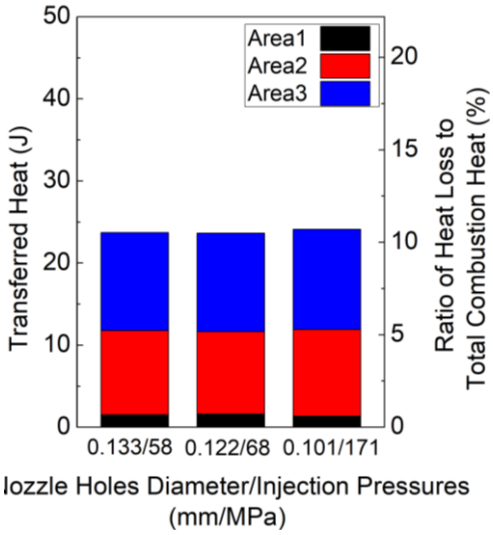

Figure 8. Heat transfer and heat loss ratio against the total combustion heat under similar injection rate conditions

ture compared to the reference oxygen concentration of 21%. Additionally, considering the impingement distance and the injection pressure effect, except for an injection pressure of 180 MPa, there were relatively minor differences in transferred heat among the different impingement distances. However, at this combined effect, a significant effect was seen at the nozzle hole diameter on the transferred heat. Specifically, larger nozzle hole diameters resulted in less heat loss at both injection pressure of 80 and 120 MPa, respectively. Contrarily, more heat loss was found for larger nozzle hole diameter at an injection pressure of 180 MPa. This suggests that controlling the heat loss can potentially be achieved by considering this combined effect while maintaining a similar injection rate.

Figure 8 presents the intriguing findings of heat transfer and its ratio of heat lost against the total combustion heat, aiming to explore the potential for achieving similar injection rates. Both the nozzle hole diameter and injection pressure were adjusted to achieve a similar injection rate of 0.133/58, 0.122/68, and 0.101/171 mm/MPa,

respectively. Notably, no significant differences were observed among all cases in terms of heat transfer. This outcome can be attributed to the similarity in injection rate profiles across the conditions. These results emphasize the effectiveness of manipulating the injection rate profile as a viable strategy for controlling the heat transfer to the wall. Specifically, at similar injection rate profiles, the heat transfer through the wall was approximately 24 Joules, while the heat loss ratio to the wall is about 11% of the total combustion energy.

CONCLUSIONS

The heat transfer in a flat-wall impinging diesel spray flame under diesel engine-like conditions has been investigated, examining various of injection pressures, nozzle hole diameters, impingement distances, and oxygen concentration effects. Following is a summary of the results of this investigation:

1. Comparing non-combustion and combustion conditions, it was determined that approximately 30-40% of the heat transfer through the wall by the convection of the non-combustion evaporating spray.
2. In case of the impingement distance and injection pressure revealed a significant increase in heat loss at an impingement distance of 50 mm and injection pressure of 180 MPa. Prior turbulent mixing effects toward the impingement to the wall have an important role in this heat loss analysis.
3. Correspond to the nozzle hole diameter and injection pressure, it was observed that increasing the nozzle hole diameter resulted in decreasing the heat loss at injection pressures of 80 and 120 MPa. It might be due to the flame temperature factor on heat loss under these conditions.
4. Analyzing the effect of oxygen concentration and injection pressure on the heat loss of the wall revealed that lower oxygen concentrations led to reduced heat loss across all injection pressures. Factors such as lower flame temperature, reduced flame contact area, and shortened contact duration influenced heat loss under these conditions.
5. Similar injection rate profiles resulted in similar heat transfer regardless of the nozzle hole diameter and injection conditions. This indicates the importance and potential of injection rate shaping for reducing wall heat loss.

ACKNOWLEDGEMENTS

We would like to thank University of Hiroshima for their support with measurement in this study.

DECLARATION OF CONFLICTING INTERESTS

The author(s) declared no potential conflicts of interest with respect to the research, authorship, and/or publication of this article.

FUNDING

The author(s) disclosed receipt of the following no financial support for the research, authorship, and/or publication of this article.

REFERENCES

[1] IEA (2022), Transport, IEA, Paris https://www.iea.org/reports/transport.
[2] IEA (2020), Car market share by powertrain in selected countries and globally, in the Stated Policies Scenario and the Sustainable Development Scenario, 2019, 2030 and 2050, IEA, Paris.
[3] Yokoyama E, Shimura M, Kamata M, et al. Simultaneous High-speed and High-resolution PIV and Heat Flux Measurements near Piston Top under Tumble Enhanced Condition. Flow Turbulence Combust 109, 1011–1037, 2022.
[4] Dejima K, and Nakabeppu O. Attempt of estimating flow characteristics from wall heat fluxes measured using a three-point micro-electro-mechanical systems sensor. International Journal of Engine Research.;22(6):1974-1984, 2021
[5] Mahmud R, Kurisu T, Nishida K, Ogata Y, Kanzaki J, Akgol O. Effects of injection pressure and impingement distance on flat-wall impinging spray flame and its heat flux under diesel engine-like condition. Advances in Mechanical Engineering. Vol.11(7), 2019.
[6] Kuboyama T, Moriyoshi Y, and Kosaka H, Heat Transfer Analysis in a Diesel Engine Based on a Heat Flux Measurement Using a Rapid Compression and Expansion Machine, SAE Tehnical paper, 2017-32-0115, p.6, 2017.
[7] Aizawa T, Kinoshita T, Akiyama S, et al. Infrared high-speed thermography of combustion chamber wall impinged by diesel spray flame. International Journal of Engine Research. Vol.23(7):1116- 1130, 2022.
[8] Binder C, Abou Nada F, Richter M, Cronhjort A, et al., "Heat Loss Analysis of a Steel Piston and a YSZ Coated Piston in a Heavy-Duty Diesel Engine Using Phosphor Thermometry Measurements," *SAE Int. J. Engines* Vol.10(4):1954-1968, 2017,
[9] Kawanabe H, Komae J, Ishiyama T. Analysis of flow and heat transfer during the impingement of a diesel spray on a wall using large eddy simulation. International Journal of Engine Research. Vol. 20(7):758-764, 2019.
[10] A. L. Pillai, R. Kai, T. Murata, T. Ikedo, R. Masuda, R. Kurose, “Numerical analysis of heat transfer characteristics of spray flames impinging on a wall under CI engine-like conditions”, Combustion and Flame Vol.239, 111615, 2022.
[11] Schmitt M, Frouzakis CE, Wright YM, Tomboulides AG, Boulouchos K. Investigation of wall heat transfer and thermal stratification under engine-relevant conditions using DNS. International Journal of Engine Research. Vol.17(1):63-75,2016.
[12] Yan Z, Levi A, Zhang Y, Sellnau M, Filipi Z, Lawler B. A numerical evaluation and guideline for thermal barrier coatings on gasoline compression ignition engines. International Journal of Engine ResearchVol.24(5):2206-2222, 2023;
[13] Fukui, K., Wakisaka, Y., Nishikawa, K., Hattori, Y. et al., "Development of Instantaneous Temperature Measurement Technique for Combustion Chamber Surface and Verification of Temperature Swing Concept," SAE Technical Paper 2016-01-0675, 2016,
[14] Wakisaka, Y., Inayoshi, M., Fukui, K., Kosaka, H. et al., "Reduction of Heat Loss and Improvement of Thermal Efficiency by Application of “Temperature Swing” Insulation to Direct-Injection Diesel Engines," SAE Int. J. Engines Vol.9(3):2016
[15] Andruskiewicz P, Najt P, Durrett R, Biesboer S, Schaedler T, Payri R. Analysis of the effects of wall temperature swing on reciprocating internal combustion engine processes. International Journal of Engine Research. Vol.19(4):461-473.2018.
[16] Uchida N. A review of thermal barrier coatings for improvement in thermal efficiency of both gasoline and diesel reciprocating engines. International Journal of Engine Research. Vol.23(1):3-19, 2022.
[17] Horibe, N., Bao, Z., Taguchi, T., Egoshi, K. et al., “Improvement of Thermal Efficiency in a Diesel Engine with High-Pressure Split Main Injection,” SAE Technical Paper

2018-01-1791, 2018.
[18] Uchida N, Watanabe H. A new concept of actively controlled rate of diesel combustion (ACCORDIC): Part II—simultaneous improvements in brake thermal efficiency and heat loss with modified nozzles. International Journal of Engine Research. Vol.20(1):34-45, 2019.
[19] Iwamoto S, Tanaka T, Eriko Matsumura E, et al, A Study for High Efficiency of Diesel Engine in the High Load Operation（Second Report-Investigation of Effects of Fuel Property on the Wall Heat Loss with Rapid and Expansion Machine-, Transactions of Society of Automotive Engineers of Japan, Vol.50 Issue 3 p. 660-665, 2019.
[20] Mahmud R, Kurisu T, Nishida K, and et al., Experimental study on flat-wall impinging spray flame and its heat flux on wall under diesel engine–like condition: First report—effect of impingement distance. Proceedings of the Institution of Mechanical Engineers, Part D: Journal of Automobile Engineering, Vol.233(8):2187-2202, 2019.
[21] Safiullah, Ray S.C., Nishida, K., McDonell, V.G. et al., Evaluation of multi-hole diesel injectors spray under evaporating conditions: Effects of adjacent spray plumes on the macroscopic and mixture characteristics of target spray. Proceedings of the Institution of Mechanical Engineers, Part D: Journal of Automobile Engineering. 2022.
[22] Safiullah, Nishida, K., Ogata, Y. et al., Effects of nozzle hole size and rail pressure on diesel spray and mixture characteristics under similar injection rate profile–experimental, computational and analytical studies under non-evaporating spray condition. Proceedings of the Institution of Mechanical Engineers, Part D: Journal of Automobile Engineering, 236(2-3), 310-321, 2022.
[23] Safiullah, Nishida, K., & Ogata, Y. Evaporation and mixture formation characteristics of diesel spray under various nozzle hole size and injection pressure condition employing similar injection rate profile. International Communications in Heat and Mass Transfer, 123, 105184, 2021.
[24] Safiullah, Mahmud R, Nishida K, et al., EXPERIMENTAL AND COMPUTATIONAL STUDY OF DIESEL SPRAY UNDER NONEVAPORATING AND EVAPORATING CONDITIONS-EFFECTS OF NOZZLE HOLE DIAMETER AND INJECTION PRESSURE, Atomization and Sprays, Vol. 30, Issue 9, pp. 627-649, 2020.
[25] Z. Wang, S. Wu, Y. Huang, Y. Chen, and et al., "Evaporation and ignition characteristics of water emulsified diesel under conventional and low temperature combustion conditions," Energies, vol. 10, no. 8, 2017.
[26] Nakata M, Arai N, Maeda S, et al, A Study on the Wall Heat Loss in Diesel Spray Flame (Sixth Report) (Effects of Impingement Distance and Inclination Angle of the Wall on the Heat Flux), 2017 JSAE Annual Congress (Spring), No.3-17, 2017. In Japanese
[27] Aizawa T, Harada T, Kondo K, et al. Thermocouple temperature measurements in diesel spray flame for validation of in-flame soot formation dynamics. International Journal of Engine Research, 18(5-6):453-46, 2017.
[28] Akop MZ, Zama Y, Furuhata T, et al. Characteristics of adhesion diesel fuel on an impingement disk wall. Part 3: ambient pressure effect. Atomization and Sprays, Vol.24: issue 7, pp. 625–650, 2014.
[29] T. Tatsumi, S. Maeda, M. Nakata, Y. Kobashi, and et al., "A Study on the Wall Heat Loss in Diesel Spray Flame (Fourt Report: Effect of Nozzle Hole Diameter on the Heat Flux)," JSAE Trans., vol. 49, no. 2, pp. 144–149, 2018. In Japanese
[30] Mahmud, R., Nishida, K., Ogata, Y., at al. Characteristics of wall heat transfer from impinging diesel spray flame in low oxygen concentration ambient. IOP Conference Series: Materials Science and Engineering, 1010(1), 012003, 2021.